International Geology Review, Vol. 44, 2002, p. 559–574.

Geochemical and Sr-Nd Isotopic Characteristics of Late Paleogene Ultrapotassic Magmatism in Southeastern Tibet

XIAN-HUA LI,[1]

Guangzhou Institute of Geochemistry, Chinese Academy of Sciences, P.O. Box 1131, Guangzhou 510640, Guangdong, China and Department of Geosciences, National Taiwan University, Taipei 106-17, Taiwan

HANWEN ZHOU,

Guangzhou Institute of Geochemistry, Chinese Academy of Sciences, P.O. Box 1131, Guangzhou 510640, Guangdong, China

SUN-LIN CHUNG, CHING-HUA LO,

Department of Geosciences, National Taiwan University, Taipei 106-17, Taiwan

GANGJIAN WEI, YING LIU,

Guangzhou Institute of Geochemistry, Chinese Academy of Sciences, P.O. Box 1131, Guangzhou 510640, Guangdong, China

AND CHI-YU LEE

Department of Geosciences, National Taiwan University, Taipei 106-17, Taiwan

Abstract

Geochemical and Sr-Nd isotopic data are reported for late Paleogene potassic lamprophyres from western Yunnan, southeastern margin of the Tibetan Plateau. These lamprophyres are mostly ultrapotassic in composition with K_2O/Na_2O = 2.1 to 5.2, except for a few samples with shoshonitic affinity showing slightly lower K_2O/Na_2O = 1.6 to 1.7. They are characterized by high initial $^{87}Sr/^{86}Sr$ ratios of 0.70624 to 0.70924; negative $\varepsilon Nd(T)$ values of –1.7 to –4.6; enrichment in large-ion lithophile elements, light rare-earth elements, and Pb; and depletion in high-field-strength elements, resembling those of high K/Ti and low-Ti potassic magmas formed in subduction-related settings. These lamprophyres were generated by partial melting of a metasomatized, phlogopite-bearing spinel harzburgite lithospheric mantle source, followed by crystal fractionation and varying degrees of crustal assimilation. Relatively constant incompatible trace element ratios, such as Rb/Sr (~0.2), Rb/Ba (~0.1), La/Sm (~5), Th/K (~0.0003), and Nb/La (~0.2), and limited Sr and Nd isotopic compositions in the ultrapotassic rocks possibly reflect an evenly distributed metasomatized mantle source. With a general similarity in geochemistry, the potassic and ultrapotassic magmas from southeastern (40–30 Ma) and northern (<15 Ma) parts of the Tibetan Plateau display obvious differences in Th/U, Rb/Sr, and Sr-Nd isotopes. These differences in geochemistry and Sr-Nd isotopes suggest contrasting subcontinental lithosphere mantle bulk compositions beneath the southeastern and northern parts of the Tibetan Plateau, caused by metasomatism involving subducted sediments from distinct crustal provenances.

Introduction

POTASSIC IGNEOUS ROCKS, although volumetrically insignificant, occur in almost all tectonic settings except for mid-ocean ridges. In general, they may be grouped into two main categories: (1) those formed at destructive plate margins including continental arcs, oceanic arcs, and post-collisional arcs; and (2) those formed in continental and oceanic intraplate settings (e.g., Müller and Groves, 1995). It is now widely accepted that mafic potassic magmas are mostly formed by small degrees of melting of either metasomatized subcontinental lithospheric mantle (SCLM), or of metasomatic veins within the SCLM (e.g. Wyllie and Sekine, 1982; McKenzie, 1989; Foley, 1992; Rogers, 1992; Sheppard and Taylor, 1992; Gibson et al., 1993; Zhao et al., 1995; Canning et al., 1996; Turner et al., 1996; Rogers et al., 1998). Such melts, therefore, provide an important window into the composition of the SCLM.

[1]Corresponding author; email: lixh@gig.ac.cn

The collision of India with Asia since the Early Cenozoic has created the Tibetan Plateau, which is characterized by widespread post-collisional, potassic magmatism (e.g., Tuner et al., 1993, 1996; Chung et al., 1998). In the northern and western portion of the Plateau, postassic magmatism has been active since ~25 Ma, and has been the subject of intensive study (e.g., Arnaud et al., 1992; Tuner et al., 1993, 1996; Miller et al., 1999). In contrast, in the eastern portion of the Plateau, potassic magmatism was active between 40 and 30 Ma (Chung et al., 1998), and only limited geochemical data are available (Zhang et al., 1987; Zhu et al., 1992). To provide a more comprehensive data set of geochemical characteristics and place better constraints on the composition of the SCLM beneath the southeastern margin of the Tibetan Plateau, this paper presents a detailed geochemical and Sr-Nd isotopic study of the Late Paleogene potassic lamprophyres around the Diancang Shan–Ailao Shan shear zone in western Yunnan (South China).

Geological Background and Lamprophyre Petrography

The Ailao Shan–Diancang Shan Shear zone is a major segment of the Red River shear zone that extends over 1000 km from the eastern end of the Himalayan syntaxis in western Yunnan Province (South China) to the Tonkin Gulf, northern Vietnam (Fig. 1). It represents the most pronounced morphologic and geologic discontinuity in Southeast Asia that resulted from the collision of India with Asia (e.g., Tapponnier et al., 1982). Along this shear zone, the Indochina Block extruded ~600 km southeastward relative to the South China Block in mid-Tertiary time (Leloup et al., 1995; Chung et al., 1997; Wang et al., 1998). This large-scale continental extrusion was preceded by the occurrence of widespread potassic magmatism in the eastern Tibetan Plateau, ascribed to an intraplate extension setting in the region resulting from convective removal of the thickened Asian lithospheric mantle (Chung et al., 1997, 1998).

In western Yunnan, WNW-trending potassic to ultrapotassic lamprophyric dikes occur extensively to both sides of the Ailao Shan-Diancang Shan shear zone (Fig. 1). Previous ^{40}Ar-^{39}Ar dating for six mica separates indicated that lamprophyres from the study area were emplaced at 33–34 Ma, coeval with the potassic magmatism of 30–40 Ma in eastern Tibet (Chung et al., 1998). All the lamprophyric dikes are undeformed and are intruded into pre-Cenozoic country rocks. The thickness of the dikes varies from 0.4 to 1.5 m. In general, they were intruded along joint planes in the country rocks against which some of them have chilled margins. The lamprophyre dikes show typical porphyritic textures, with phlogopite as the dominant phenocrysts in a glassy to fine-grained groundmass. Large (1–4 mm), euhedral phlogopite phenocrysts are set in a groundmass of mainly felsic components. Four petrographic types of lamprophyres can be distinguished in terms of phenocryst mineralogy: (1) phlogopite phyric; (2) phlogopite-clinopyroxene phyric; (3) phlogopite-apatite phyric; and (4) phlogopite-amphibole phyric. Most clinopyroxene phenocrysts are surrounded by secondary amphibole.

Phenocryst mineralogy is dominated by large phlogopites with variably high Mg# values of 0.77 to 0.87, variable TiO_2 (0.73–1.57%) and Al_2O_3 (12.5–13.5%) contents (Table 1). The clinopyroxene phenocrysts are euhedral, with variably high MgO (15.76–19.16%) and CaO (18.14–23.92%) contents. Amphibole phenocrysts are characterized by high MgO content (19.9%). Plagioclase feldspars are sodium rich, with Na_2O contents of 5.2–5.7%. The groundmass minerals are mainly orthoclase, plagioclase, apatite, fine-grained phlogopite, and quartz. Alteration products consist mainly of epidote, clays, or carbonate replacement after saussuritization. Among the potassic rocks in the study area, the lamprophyres are the most mafic. Thus, they are considered appropriate to be used in constraining the regional SCLM compositions.

Analytical Method

Major-element oxides were determined using a Rigaku RIX 2000 X-ray fluorescence spectrometer (XRF) at the Department of Geosciences, National Taiwan University, following the procedures of Lee et al. (1997). Analytical uncertainties are generally better than 1%–5%. Trace elements were analyzed using a Perkin-Elmer ELAN 6000 inductively coupled plasma mass spectrometer (ICP-MS) at the Guangzhou Institute of Geochemistry, Chinese Academy of Sciences. Detailed procedures for trace-element analysis by ICP-MS were described by Li (1997). An internal standard solution containing the single element Rh was used to monitor signal drift during counting. The international standard BCR-1 was chosen to calibrate element concentrations of measured samples. Analytical precision for

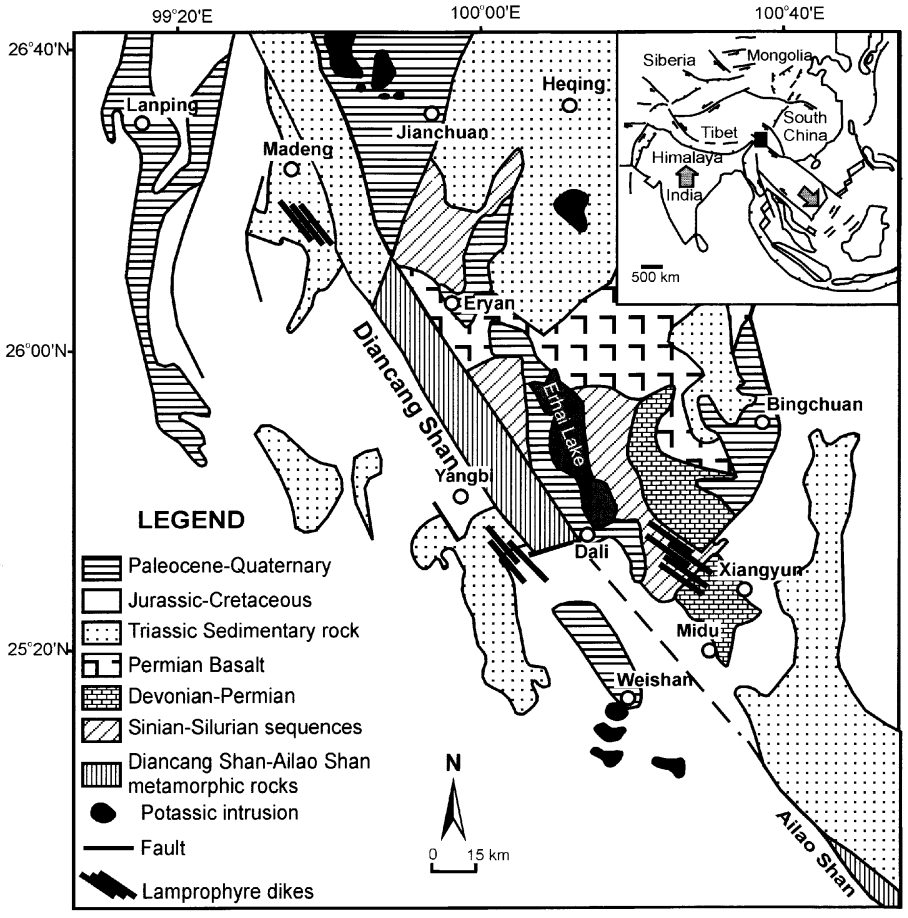

FIG. 1. Simplified geological map of western Yunnan Province (modified after Bureau of Geology and Mineral Resources of Yunnan Province, 1990), showing the distribution of Late Paleogene lamprophyres. The inset is a tectonic sketch map of Southeast Asia, modified after Tapponnier et al. (1982).

most elements is better than 3%. Sr isotopic compositions were determined using a VG-354 mass spectrometer operated in dynamic multi-collector mode at Guangzhou Institute of Geochemistry. Nd isotopic compositions were determined using a Finnigan MAT-262 mass spectrometer operated in a static multi-collector mode at the Research Center of Geoscience, Chinese Academy of Sciences in Beijing. The $^{87}Sr/^{86}Sr$ ratio of the NBS 987 standard and $^{143}Nd/^{144}Nd$ ratio of the La Jolla standard measured during this study were 0.710310 ± 15 ($2\sigma_m$) and 0.511852 ± 8 ($2\sigma_m$), respectively. The measured $^{87}Sr/^{86}Sr$ and $^{143}Nd/^{144}Nd$ ratios are normalized to $^{86}Sr/^{88}Sr = 0.1194$ and $^{146}Nd/^{144}Nd = 0.7219$, respectively.

Results

Major and trace elements

Seventeen least-altered potassic lamphrophyre samples from western Yunnan were collected for major- and trace-element analyses. Results are presented in Table 2. All of the samples are alkaline and range from trachy-basaltic to trachytic composition in terms of a total alkalis-silica plot (Fig. 2A). Most samples have an ultra-potassic character, with $K_2O/Na_2O = 2.1$ to 5.2, except for two samples (96YN137 and 96YN142) having slightly lower $K_2O/Na_2O = 1.6$ to 1.7, which therefore fall in the shoshonitic field (Fig. 2B). Overall, the studied potassic lamphrphyre samples range from relatively

TABLE 1. Microprobe Analyses of Phenocrysts in Ultrapotassic Lamprophyres from Southeastern Tibet (western Yunnan, South China)[1]

	Mica				Clinopyroxene						Amphibole	K-feldspar	
Sample no.:	99YN132	99YN135	99YN137	99YN140	99YN132			99YN137	99YN140	99YN135	99YN132	99YN135	
							wt%						
SiO_2	39.80	40.87	39.72	40.68	54.05	53.28	52.78	52.82	54.04	54.78	54.63	64.27	65.53
TiO_2	0.81	1.57	0.73	1.31	0.14	0.11	0.15	0.16	0.09	0.04	0.47	0.02	0.03
Al_2O_3	13.03	12.69	13.21	13.22	0.60	0.78	0.80	0.82	0.78	0.77	1.89	18.70	18.75
FeO	9.50	7.20	12.09	7.99	3.77	3.93	6.66	5.90	3.43	5.61	8.24	0.30	0.29
MnO	0.09	0.03	0.12	0	0.09	0.08	0.20	0.22	0.06	0.22	0.29	0.00	0.01
MgO	21.13	22.19	18.58	21.86	18.55	18.11	15.76	16.49	17.86	19.16	19.86	0.00	0.00
CaO	0.01	0.03	0.02	0.06	22.44	22.52	23.64	23.78	23.92	18.14	10.73	0.15	0.20
Na_2O	0.46	0.32	0.07	0.11	0.39	0.45	0.57	0.53	0.44	0.31	1.59	5.55	5.24
K_2O	10.03	9.81	9.62	10.4	0.00	0.03	0.00	0.00	0.02	0.07	0.33	10.04	10.47
Total	94.86	94.71	94.16	95.63	100.03	99.29	100.56	100.72	100.64	99.10	98.03	99.03	100.52
Ox. form, atoms	2	22	22	22	6	6	6	6	6	6	23	8	8
Si	5.82	5.90	5.90	5.86	1.97	1.96	1.95	1.94	1.96	2.00	7.69	2.96	2.97
Ti	0.08	0.18	0.08	0.14	0.00	0.00	0.01	0	0.00	0.00	0.05	0.00	0.00
Al	2.24	2.16	2.32	2.24	0.03	0.03	0.04	0.04	0.03	0.04	0.31	1.01	1.00
Fe	1.16	0.88	1.50	0.96	0.11	0.12	0.20	0.18	0.10	0.17	0.97	0.01	0.01
Mn	0.02	0.00	0.02	0.00	0.00	0.00	0.01	0.01	0.00	0.01	0.03	0.00	0.00
Mg	4.62	4.78	4.12	4.70	1.01	0.99	0.87	0.9	0.97	1.05	4.17	0.00	0.00
Ca	0.00	0.00	0.00	0.00	0.88	0.89	0.94	0.94	0.93	0.71	1.62	0.01	0.01
Na	0.14	0.10	0.02	0.04	0.03	0.03	0.04	0.04	0.03	0.02	0.44	0.50	0.46
K	1.88	1.80	1.82	1.90	0.00	0.00	0.00	0	0.00	0.01	0.06	0.59	0.60
Total	15.96	14.00	15.78	15.84	4.03	4.02	4.05	4.05	4.02	3.99	15.34	5.08	5.05
Mg#	0.82	0.87	0.76	0.85	0.91	0.91	0.83	0.85	0.92	0.88	0.84		

Mg# = $Mg/(Mg + Fe^{2+})$, assuming $Fe_2O_3/(FeO + Fe_2O_3) = 0.20$. Total iron as FeO. Ox. form = oxygen formula. Samples were analyzed in the Analytical Center of the China University of Geosciences (Wuhan).

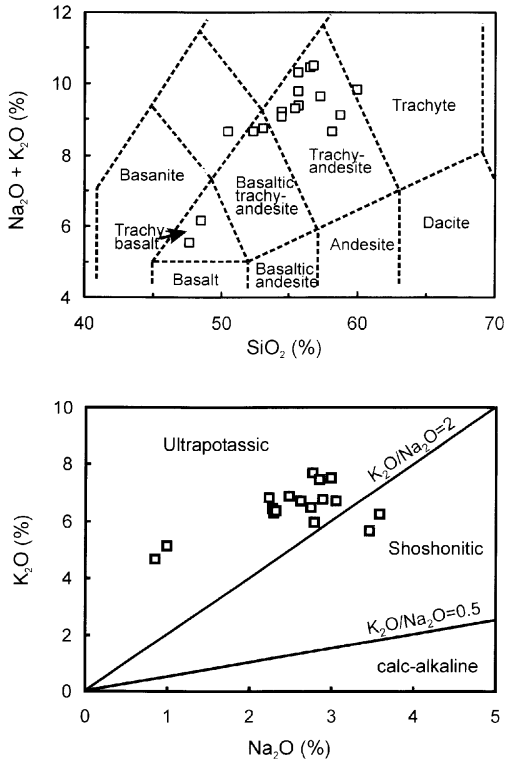

FIG. 2. Potassic lamphrophyre samples from the southeastern Tibetan Plateau plotted on (A) a total alkalis versus SiO_2 diagram for classification, and (B) a K_2O versus Na_2O diagram showing that they are ultrapotassic or shoshonitic in character.

primitive to evolved compositions with 0.73 to 0.65 for Mg# value, 415 to 153 ppm for Cr, and 244 to 71 ppm for Ni. Two samples (96YN140 and 96YN143) have high MgO (14.9%–16.3%), Cr (>1000 ppm), and Ni (>400 ppm), indicating accumulation of clinopyroxene. SiO_2 and Al_2O_3 increase, whereas Ti_2O, CaO, Fe_2O_3, and P_2O_5 decrease, with decreasing MgO for all but two cumulate samples (Fig. 3), indicating fractional crystallization of clinopyroxene, Ti-Fe oxides, and apatite, but not plagioclase. The sum of K_2O + Na_2O is relatively constant between 8.6% and 10.3%.

The compatible trace elements, Ni, Cr, V, Sc, and Co correlate positively with MgO, Fe_2O_3, and CaO, and negatively with SiO_2, again indicative of fractionation dominated by clinopyroxene. All of the samples are characterized by variable enrichment of incompatible trace elements. Most incompatible trace elements, such as La, Nb, and Th, increase with decreasing MgO, being fractionation related (Fig. 4). Rb concentrations provide an exception to such a negative correlation predicted by crystal fractionation, with a relatively constant concentration of 200–250 ppm over a range of MgO, consistent with phlogopite removal during fractionation. The abundance of Sr is very high, ranging from 900 to 1700 ppm, and shows a weakly positive correlation with MgO apart from the two cumulate samples (Fig. 4). All of the lamprophyre samples show similar REE patterns characterized by moderate enrichment of LREE (La = 22-44 ppm and La/Yb = 14–24 being negatively correlated with MgO [Fig. 4]), flat HREE distribution, and moderate Eu anomalies (Eu/Eu* = 0.77–0.86) (Fig. 5).

On a primitive mantle–normalized incompatible-element diagram (Fig. 6), all of the potassic rocks show similar patterns, being enriched in large-ion lithophile elements (LILE: Rb, Ba, Th, U, Sr, and K), LREE and Pb, and depleted in high-field-strength elements (HFSE: Nb, Ta, Zr, Hf and Ti) rel-

TABLE 2. Chemical Analyses of Potassic rocks from Southeastern Tibet (western Yunnan, South China) [1]

Sample:	96YN131	96YN132	96YN133	96YN134	96YN135	96YN136
			Major elements, wt%			
SiO_2	55.69	54.39	56.57	56.79	52.40	55.62
TiO_2	0.66	0.70	0.57	0.57	0.74	0.61
Al_2O_3	13.58	12.61	13.91	14.13	12.39	13.88
Fe_2O_3*	6.30	6.68	4.99	5.58	6.75	6.27
MnO	0.11	0.11	0.09	0.09	0.12	0.09
MgO	6.32	7.16	4.98	4.53	6.38	5.02
CaO	4.61	5.63	5.13	4.04	6.27	4.29
Na_2O	3.07	2.75	2.77	3.00	2.31	2.86
K_2O	6.70	6.44	7.67	7.48	6.32	7.43
P_2O_5	0.53	0.62	0.46	0.42	0.66	0.51
Mg#	0.70	0.71	0.70	0.66	0.69	0.65
			Trace elements, ppm			
Sc	12.0	14.1	12.2	10.4	15.4	11.7
V	121	132	106	99.5	126	114
Cr	218	262	165	153	264	161
Co	23.4	25.7	14.2	16.2	25.7	20.2
Ni	136	165	97.1	99.5	171	109
Cu	117	45.1	95.5	147	115	130
Zn	59.3	71.3	56.5	59.5	78.6	50.8
Ga	16.3	15.8	16.8	17.5	16.0	16.4
Ge	1.30	1.32	1.22	1.23	1.30	1.19
Rb	245	233	250	174	227	246
Sr	1087	1418	1006	1047	1088	1532
Y	22.6	23.0	22.7	23.5	24.5	21.6
Zr	71.8	95.6	82.3	102	86.7	90.6
Nb	8.92	8.44	9.71	12.0	9.05	7.89
Cs	5.07	5.39	5.08	3.93	5.85	4.82
Ba	2148	2989	2204	2076	2038	2862
La	39.6	38.8	39.9	44.1	43.1	41.3
Ce	77.0	75.4	76.3	81.8	84.7	75.6
Pr	9.90	9.90	9.71	10.1	10.6	9.55
Nd	38.9	39.3	37.6	37.9	42.5	36.5
Sm	7.59	7.85	7.32	7.48	8.37	7.23
Eu	1.95	1.91	1.84	1.89	2.15	1.91
Gd	6.34	6.66	5.99	5.95	6.97	6.03
Tb	0.87	0.89	0.84	0.87	0.96	0.82
Dy	4.57	4.60	4.44	4.66	4.98	4.30
Ho	0.84	0.85	0.84	0.87	0.91	0.80
Er	2.41	2.43	2.38	2.52	2.54	2.30
Tm	0.32	0.33	0.33	0.36	0.34	0.31
Yb	2.13	2.08	2.16	2.33	2.22	1.98
Lu	0.31	0.31	0.32	0.35	0.33	0.29
Hf	2.18	2.83	2.51	3.13	2.55	2.61
Ta	0.60	0.61	0.72	0.91	0.63	0.56
Pb	33.2	24.5	32.3	28.5	36.6	21.7
Th	15.3	15.5	18.7	21.2	16.2	14.8
U	5.34	5.26	6.57	8.34	5.90	5.29

Table continues

TABLE 2. *Continued*

Sample:	96YN137	96YN138	96YN139	96YN140	96YN141	96YN142
			Major elements, wt%			
SiO_2	58.68	58.18	57.28	48.56	50.58	59.93
TiO_2	0.56	0.58	0.60	0.55	0.86	0.50
Al_2O_3	14.61	13.19	14.25	9.97	11.88	15.04
Fe_2O_3*	5.52	5.23	5.91	7.79	8.44	4.00
MnO	0.09	0.14	0.10	0.14	0.10	0.08
MgO	4.52	5.46	5.24	14.93	9.72	4.15
CaO	3.96	4.78	3.66	7.05	6.68	4.52
Na_2O	3.46	2.31	2.90	0.99	2.32	3.59
K_2O	5.66	6.31	6.74	5.14	6.32	6.23
P_2O_5	0.43	0.49	0.47	0.48	0.77	0.34
Mg#	0.66	0.71	0.67	0.82	0.73	0.71
			Trace elements, ppm			
Sc	9.55	11.5	8.82	16.5	14.5	9.73
V	111	90.6	111	138	136	68.8
Cr	'222	195	160	1022	415	164
Co	16.8	15.5	18.4	44.4	33.5	11.8
Ni	78.6	127	105	433	244	71.3
Cu	24.2	13.0	52.7	68.1	77.9	67.4
Zn	57.5	79.9	45.3	75.6	57.8	47.6
Ga	17.9	15.2	17.2	10.4	14.0	17.8
Ge	1.55	1.35	1.20	1.26	1.28	1.23
Rb	230	213	240	221	259	232
Sr	1085	936	1211	1323	1735	1057
Y	21.2	19.8	23.4	16.7	19.6	20.9
Zr	206	148	81.9	97.9	104	92.7
Nb	9.27	9.21	10.7	4.61	7.28	11.2
Cs	6.99	11.4	4.99	22.1	27.0	6.37
Ba	3419	2144	2116	1748	4315	3104
La	41.5	36.9	40.7	23.0	33.4	43.4
Ce	81.7	68.1	80.3	46.5	64.3	83.8
Pr	9.87	8.63	10.1	6.14	8.45	10.5
Nd	37.5	33.2	38.9	25.6	33.7	39.4
Sm	6.92	6.44	7.60	5.21	6.79	7.53
Eu	1.86	1.59	1.93	1.32	1.67	1.77
Gd	5.95	5.38	6.33	4.51	6.18	6.07
Tb	0.80	0.75	0.89	0.61	0.77	0.83
Dy	4.10	3.91	4.62	3.26	3.95	4.27
Ho	0.75	0.72	0.86	0.61	0.73	0.76
Er	2.10	2.06	2.48	1.76	2.04	2.13
Tm	0.31	0.29	0.34	0.24	0.27	0.28
Yb	1.99	1.89	2.15	1.60	1.74	1.80
Lu	0.30	0.29	0.32	0.25	0.26	0.27
Hf	5.59	4.06	2.42	2.47	2.70	2.55
Ta	0.68	0.69	0.75	0.30	0.51	0.70
Pb	43.7	50.1	23.1	181	15.7	31.7
Th	16.9	20.4	19.0	8.53	13.5	14.9
U	6.57	9.34	6.79	2.98	4.65	5.57

Table continues

TABLE 2. *Continued*

Sample:	96YN143	96YN144	96YN145	96YN146	96YN147
			Major elements, wt%		
SiO_2	47.77	53.12	55.52	54.46	55.40
TiO_2	0.57	0.83	0.71	0.67	0.66
Al_2O_3	9.48	12.30	13.14	13.16	13.09
Fe_2O_3*	8.32	7.12	7.00	6.36	6.16
MnO	0.15	0.12	0.10	0.11	0.10
MgO	16.32	8.30	7.09	6.05	6.72
CaO	6.88	6.66	5.56	5.29	4.64
Na_2O	0.86	2.79	2.49	2.24	2.63
K_2O	4.65	5.95	6.88	6.81	6.68
P_2O_5	0.49	0.73	0.59	0.68	0.56
Mg#	0.82	0.73	0.70	0.69	0.72
			Trace elements, ppm		
Sc	18.8	15.6	13.5	14.1	14.2
V	141	138	140	119	116
Cr	1050	338	243	205	224
Co	49.4	28.6	23.8	21.3	24.0
Ni	503	170	152	119	147
Cu	37.0	14.8	51.1	44.6	95.5
Zn	78.8	69.9	61.6	82.4	55.1
Ga	10.3	14.8	16.0	15.4	16.2
Ge	1.31	1.39	1.29	1.36	1.19
Rb	223	233	255	257	138
Sr	996	1267	1215	1448	918
Y	16.7	26.0	23.9	21.6	13.5
Zr	92.5	88.7	92.2	170	83.6
Nb	4.42	8.40	8.67	8.35	10.4
Cs	26.7	6.71	5.85	14.7	4.76
Ba	1658	1653	2483	2491	1774
La	22.4	35.7	41.2	42.5	33.7
Ce	44.7	70.9	77.5	81.8	70.8
Pr	6.09	9.47	10.3	10.5	8.24
Nd	25.4	38.2	39.9	41.3	32.5
Sm	5.25	8.00	7.93	8.29	6.39
Eu	1.36	2.03	1.99	2.03	1.54
Gd	4.55	7.06	6.76	6.55	5.50
Tb	0.61	0.99	0.91	0.86	0.75
Dy	3.25	5.21	4.71	4.30	3.95
Ho	0.61	0.94	0.86	0.77	0.72
Er	1.76	2.56	2.46	2.17	2.07
Tm	0.24	0.34	0.33	0.29	0.28
Yb	1.55	2.14	2.16	1.87	1.83
Lu	0.24	0.32	0.32	0.28	0.27
Hf	2.41	3.18	2.72	4.40	2.57
Ta	0.30	0.54	0.58	0.55	0.75
Pb	123	24.8	19.0	21.5	26.0
Th	8.11	9.28	14.6	18.8	15.9
U	2.76	3.28	5.21	6.74	6.71

[1]Mg# = $Mg/(Mg + Fe^{2+})$, assuming $Fe_2O_3/(FeO + Fe_2O_3) = 0.20$. Total iron as Fe_2O_3.

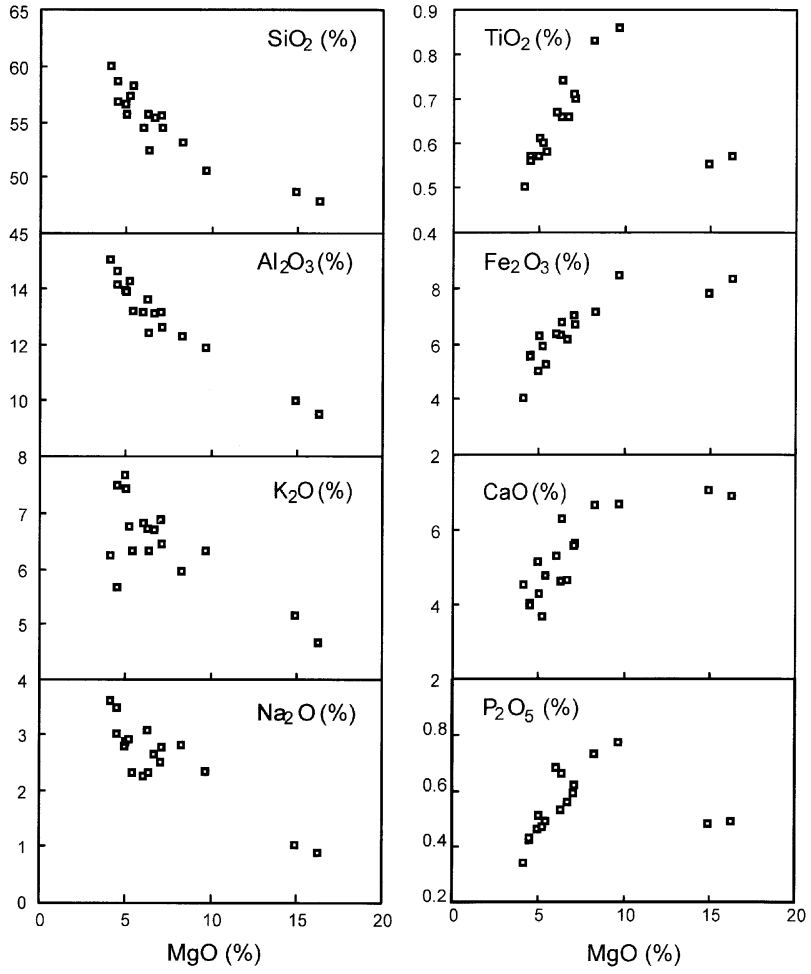

FIG. 3. Major element versus MgO variation diagrams, illustrating the compositional range of the southeastern Tibetan ultrapotassic lamphrophyres.

ative to neighboring elements. These geochemical features are of typical for high K/Ti and low-Ti potassic magmas formed in subduction-related environments, in contrast to low K/Ti and high-Ti potassic magmas formed in intraplate settings (Rogers, 1992).

Sr-Nd isotopes

All investigated samples were analyzed for Sr and Nd isotopic compositions in this study (Table 3). Overall, the potassic lamprophyres have a relatively small range of Sr and Nd isotopic compositions, with initial $^{87}Sr/^{86}Sr$ ratios ranging from 0.70624 to 0.70924, and initial εNd values ranging from –1.73 to –4.58. Initial Sr and Nd isotopes show a weakly negative correlation on a conventional εNd(T) versus $(^{87}Sr/^{86}Sr)_i$ diagram (Fig. 7).

Discussion

Petrogenesis

High values of K and Na for the southeastern Tibetan potassic lamprophryres imply derivation from an alkali-enriched mantle source. K_2O is extremely high regardless of the contents of SiO_2 (50 to 60%) and MgO (9.7 to 4.2%) for all but the two cumulate-enriched samples, reflecting control by a potassic phase not only during fractionation but also

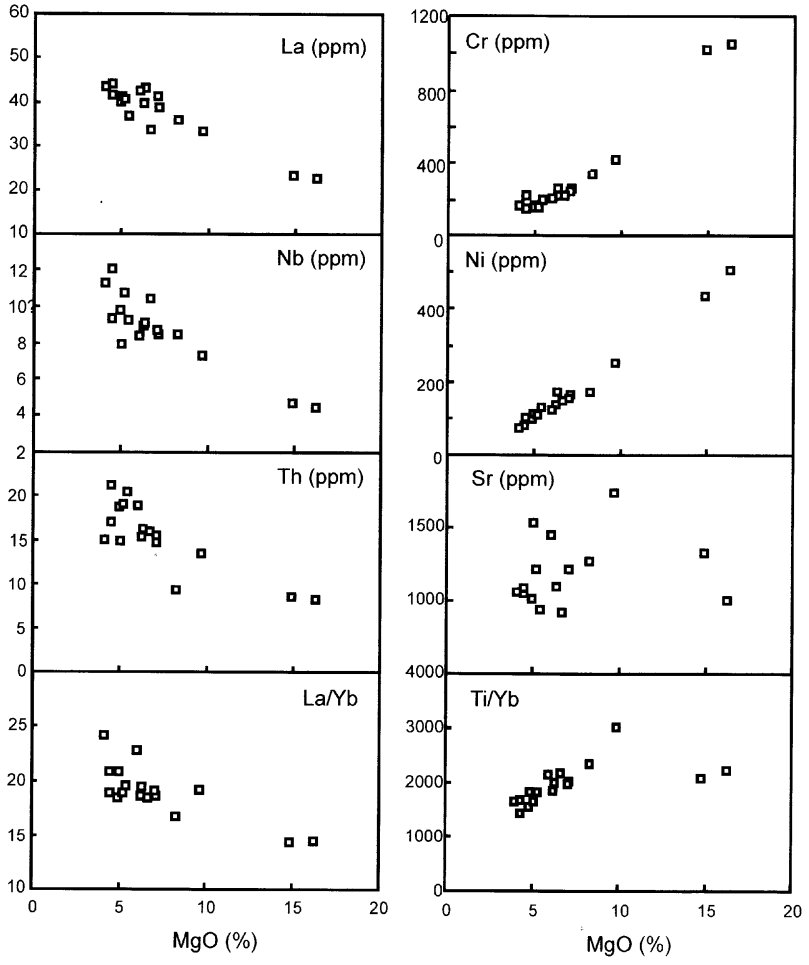

FIG. 4. Selected trace-element abundances and ratios versus MgO variation diagrams for the southeastern Tibetan ultrapotassic lamphrophyres.

in the mantle source. The majority of studied ultrapotassic samples have high, constant K_2O/Na_2O ratios of 2–3, except for two cumulate samples ($K_2O/Na_2O > 5$) and two evolved shoshonitic samples ($K_2O/Na_2O = 1.6–1.7$, MgO = 4.2–4.5%). Thus, the high K_2O in the lamprophyres is a primary feature, indicating the presence of a potassic phase, most likely phlogopite, in their source region. The origin of potassic-rich alkaline mafic magmas by partial melting of a phlogopite-bearing metasomatized mantle source has been well established by Wyllie and Sekine (1982). Such magmas should be enriched in K and Ba, as found in the studied lamprophyre samples. There are fairly constant incompatible element ratios, such as Rb/Sr (~0.2), Rb/Ba (~0.1), La/Sm (~5), Th/K (~0.0003), and Nb/La (~0.2) and limited Sr and Nd isotopic compositions in the lamprophyre samples. This probably reflects generation of a source where metasomatic products are possibly evenly distributed, rather than a heterogeneously-vented mantle. It is noteworthy that these potassic lamprophyres have relatively low, constant La/Sm (4.3–6.0) and La/Yb (17–24) ratios and flat HREE patterns, compared to the northern Tibetan shoshonitic rocks with variably high La/Sm (6.5–32.5) and La/Yb (10–170) ratios and depleted REEE (Tuner et al., 1996). Flat HREE patterns in the southeastern Tibetan ultrapotassic rocks are

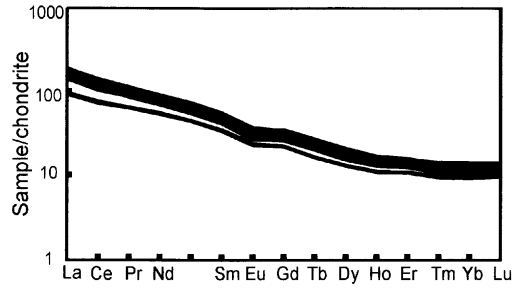

FIG. 5. Chondrite-normalized REE diagrams for the southeastern Tibetan potassic lamphrophyres. The normalization values are from Sun and McDonough (1989).

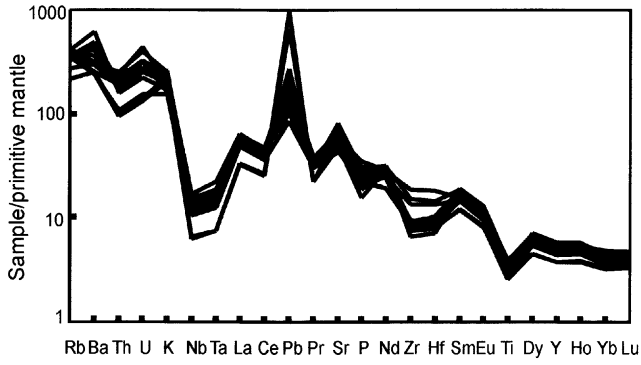

FIG. 6. Primitive mantle–normalized incompatible-element distribution diagrams for the southeastern Tibetan ultrapotassic lamphrophyres. The normalization values are from Sun and McDonough (1989).

consistent with derivation from a spinel-facies mantle, contrasting with a garnet facies mantle source invoked for northern Tibetan shoshonitic rocks (Turner et al., 1996). Limited ranges of La/Sm and La/Yb in the studied ultrapotassic lamphrophyres demonstrate that geochemical variations are mostly attributed to fractionation, rather than partial melting.

Although the studied ultrapotassic lamprophyre samples are mostly mafic in composition, many lines of geochemical evidence suggest an important role for fractional crystallization during magma evolution. These include: (1) a broad range from relatively primitive to evolved composition (MgO = 9.7–4.2%); (2) the increase of SiO_2, Al_2O_3, LREE, and HFSE and the decrease of Ti_2O, CaO, Fe_2O_3, P_2O_5, and compatible elements with decreasing MgO (Figs. 3 and 4); (3) linear co-variations of incompatible trace elements; and (4) the overall increase in total REE contents with decreasing MgO. These characteristics indicate that potassic lamprophyres evolved predominantly through fractionation of clinopyroxene ± Ti-Fe oxides ± apatite. Negative correlation between Al_2O_3 and MgO indicates that plagioclase was not the fractionated phase. Thus, the moderate Eu negative anomaly in all samples is interpreted as inheritance from the mantle source.

Although all of the ultrapotassic lamprophyres occur as dikes showing rapid emplacement, chilled liquids, and no clear geologic evidence of crustal assimilation, geochemical and isotopic variations in the lamprophryes suggest involvement of crustal components to some degrees in the evolution of the magma. Initial $^{87}Sr/^{86}Sr$ ratios and εNd values, despite their limited variations, are negatively correlated for all but two cumulate samples (Fig. 7). Furthermore, εNd(T) values decrease with decreasing MgO for most samples (Fig. 8), indicating involvement of crustal components during the crystal fractionation of the ultrapotassic magma.

TABLE 3. Sr-Nd Isotopes of Ultrapotassic Lamprophyres from Southeastern Tibet (western Yunnan, South China)[1]

Sample	$^{87}Rb/^{86}Sr$	$^{87}Sr/^{86}Sr$	$(^{87}Sr/^{86}Sr)_i$	$^{147}Sm/^{144}Nd$	$^{143}Nd/^{144}Nd$	εNd(T)	T_{DM} (Ma)
96YN131	0.6514	0.707094 ± 10	0.70679	0.1181	0.512448 ± 10	−3.68	1.12
96YN132	0.4749	0.706845 ± 11	0.70662	0.1207	0.512443 ± 06	−3.78	1.16
96YN133	0.7184	0.706796 ± 13	0.70646	0.1179	0.512442 ± 11	−3.79	1.13
96YN134	0.4812	0.706464 ± 09	0.70624	0.1192	0.512440 ± 10	−3.83	1.14
96YN135	0.6045	0.706849 ± 12	0.70657	0.1191	0.512444 ± 07	−3.76	1.14
96YN136	0.4644	0.706644 ± 12	0.70643	0.1197	0.512444 ± 15	−3.76	1.14
96YN137	0.6135	0.708677 ± 16	0.70839	0.1115	0.512411 ± 05	−4.40	1.10
96YN138	0.6584	0.709545 ± 10	0.70924	0.1173	0.512402 ± 07	−4.58	1.18
96YN139	0.5747	0.706606 ± 10	0.70634	0.1181	0.512437 ± 09	−3.89	1.14
96YN140	0.4830	0.707578 ± 15	0.70735	0.1232	0.512543 ± 07	−1.83	1.02
96YN141	0.4315	0.707751 ± 14	0.70755	0.1215	0.512446 ± 14	−3.72	1.16
96YN142	0.6363	0.707205 ± 11	0.70691	0.1155	0.512432 ± 09	−3.99	1.11
96YN143	0.6473	0.707424 ± 11	0.70712	0.1251	0.512548 ± 13	−1.73	1.04
96YN144	0.5333	0.706497 ± 11	0.70625	0.1267	0.512467 ± 12	−3.31	1.20
96YN145	0.6068	0.706933 ± 12	0.70665	0.1201	0.512416 ± 17	−4.30	1.19
96YN146	0.5136	0.706831 ± 11	0.70659	0.1214	0.512522 ± 13	−2.24	1.04
96YN147	0.4349	0.707182 ± 10	0.70698	0.1187	0.512458 ± 09	−3.48	1.11

[1]Initial $^{87}Sr/^{86}Sr$ ratios and εNd(T) values are corrected at T = 33 Ma, the emplacement age of the lamprophyres obtained by $^{40}Ar/^{39}Ar$ dating (Chung et al., 1998). T_{DM}: Nd modal age calculated assuming a linear isotopic growth for a depleted mantle reservoir from εNd(T) = 0 at 4.55 Ga to εNd(T) = +10 ($^{143}Nd/^{144}Nd$ = 0.51315) at present with $^{147}Sm/^{144}Nd$ = 0.2137.

Absence of geochemical and isotopic compositions for the crustal contaminants and the parental magma precludes quantitative calculation for the AFC processes. However, it can be expected that assimilation of crustal contaminants with an Sr concentration of ~260 ppm for bulk crust (Taylor and McLennan, 1985) would not significantly change the Sr isotopic composition of the lamprophyres, because of very high Sr contents (900 to 1700 ppm) in the ultrapotassic lamprophyres.

Implications for the composition of the southeastern Tibetan sub-continental lithosphere mantle (SCLM)

The studied potassic lamphrophyres provide a window into the composition of the southeastern Tibetan SCLM. Most ultrapotassic samples display similar trace element patterns in a primitive mantle–normalized diagram, apart from a few samples with pronounced Nb-Ta negative and positive Pb anomalies, possibly caused by significant crustal contamination (Fig. 6). These ultrapotassic lamprophyres, particularly those with high MgO contents (>8%), require a metasomatized, phlogopite-bearing spinel harzburgite source residing in the SCLM. In this scheme, phlogopite-bearing metasomatized mantle was formed at the root of a subduction zone by hybridization between slab-derived hydrous siliceous magma and the overlying mantle wedge. Therefore, the ubiquitous enrichment of most incompatible elements, low Nb/U (1.2–2.6) and Ce/Pb (0.3–4.1) ratios, and negative Nb-Ta and Ti anomalies in the ultrapotassic lamprophyres are features of either island-arc magmas or upper-crustal sediments. Because significant involvement of crustal components to the magma was unlikely in terms of geochemical and Sr-Nd isotopic compositions, the crustal components in the ultrapotassic

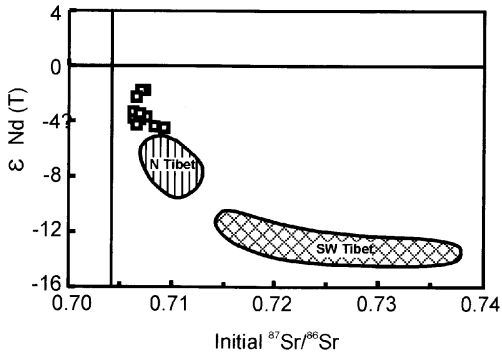

FIG. 7. Initial εNd versus $(^{87}Sr/^{86}Sr)_i$ diagram for the Tibetan potassic and ultrapotassic rocks. Data for potassic and ultrapotassic lavas from northern Tibet and southwestern Tibet are from Turner et al. (1996) and Miller et al. (1999), respectively..

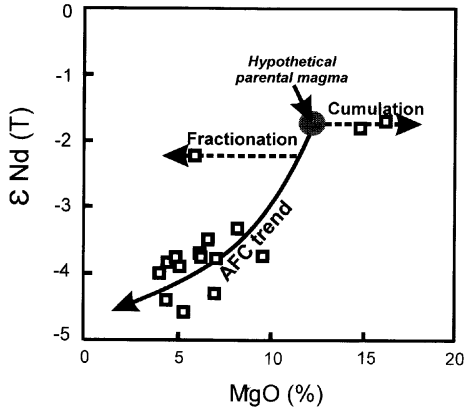

FIG. 8. Initial εNd versus MgO diagram for the southeastern Tibetan ultrapotassic lamphrophyres; εNd(T) values decrease with decreasing MgO for most samples, indicating an AFC process.

rocks are most likely inherited from the pre-existing subduction processes. These geochemical characters of arc-affinity observed in both the southeastern and northern Tibetan potassic magmas are comparable to subduction-related high K/Ti and low-Ti potassic magmas (Rogers, 1992).

Compared to the SCLM revealed by the potassic lavas in the northern Tibetan Plateau (Turner et al., 1996), the southeastern Tibetan SCLM exhibits differences in geochemistry and isotopes. The southeastern Tibetan potassic lamprophyres have a relatively low, constant Th/U ratio of 2.7 ± 0.2, consequently showing a small negative Th negative anomaly on the primitive mantle–normalized diagram (Fig. 6), in contrast to a Th/U ratio of 7–12 for the northern Tibetan potassic lavas. The unusually high Th/U ratio in the northern Tibetan lavas may not represent the Th/U ratio of the source region and the primary magma, because (1) magma generation involving only a small melt fraction in the presence of garnet may dramatically increase the Th/U ratio, and (2) the mobility of U during weathering and alteration may change the Th/U ratio (Turner et al., 1996). Nevertheless, $^{208}Pb/^{204}Pb$ ratios suggest an increase in Th/U ratios from ~3.6 to ~3.8 at 1.2 Ga for the northern Tibetan SCLM in terms of two-stage modeling of Pb isotopes (Turner et al., 1996). This is comparable with the moderate Th/U ratio of 4–5 for

typical subduction-related, high-K/Ti, low-Ti potassic magmas, as exemplified by Italian potassic lavas (Rogers, 1992). The Th/U ratios measured in the mafic samples (with <55% SiO_2) are generally considered to be representative of their mantle source, inasmuch as the D values for Th and U during melting are similar (Williams and Gill, 1989). Similarly, measured Rb/Sr ratios in the mafic samples are also similar to their source region (Rogers, 1992). The southeastern Tibetan potassic lamprophyres have Rb/Sr ratios of ~0.2, comparable with Italian potassic lavas with Rb/Sr ratios of 0.2–0.4 (Rogers, 1992), but higher than the northern Tibetan mafic potassic lavas with Rb/Sr ratios of ~0.07 (Turner et al., 1996). Differences in Th/U and Rb/Sr ratios suggest a regional geochemical contrast in the SCLM underneath the northern (<15 Ma) versus southeastern (40–30 Ma) parts of the Tibetan Plateau.

Isotopically, the southeastern Tibetan potassic lamprophyres have lower Sr and higher Nd isotopic ratios than the northern and southwestern Tibetan potassic lavas (Fig. 7). The southeastern and northern Tibetan potassic rocks are characterized by uniform Nd isotopic compositions (εNd values = –3.5 ± 0.8 and –6.5 ± 0.8, respectively) and Sm/Nd ratios ($^{147}Sm/^{144}Nd$ = 0.120 ± 0.004 and 0.080 ± 0.008, respectively). The southeastern Tibetan potassic rocks, with $^{147}Sm/^{144}Nd$ ratios close to the average value of ~0.118 for upper crust (Jahn and Condie, 1995), have Nd modal ages (T_{DM}) of 1.12 ± 0.05 Ga relative to a depleted mantle source (assuming its present-day εNd = +10 evolved since 4.0 Ga)(Table 2). The northern Tibetan potassic lavas have T_{DM} ages of 0.96 ± 0.07 Ga, but these T_{DM} ages based on the measured Sm/Nd ratios are clearly underestimated since their $^{147}Sm/^{144}Nd$ ratios (0.06–0.09) were significantly fractionated during magma genesis in the presence of garnet. Thus, Turner et al (1996) re-calculated T_{DM} ages of ~1.2 Ga for the SCLM source, assuming a 30% decrease in the Sm/Nd ratio during melting, and thus the mantle source had a $^{147}Sm/^{144}Nd$ ratio of ~0.11. This calculated $^{147}Sm/^{144}Nd$ ratio is still about 10% lower than those of the average upper crust (0.118) and the southeastern Tibetan SCLM (0.12) revealed by the ultrapotassic lamprophyres. If the northern Tibetan SCLM had the same $^{147}Sm/^{144}Nd$ ratio of ~0.12 as the southeastern Tibetan SCLM, a 50% decrease in the Sm/Nd ratio during melting wo;uld be required for the northern Tibetan potassic lavas. If this is true, the northern Tibetan SCLM should have T_{DM} ages of ~1.4 Ga. Thus, T_{DM} ages of the northern Tibetan potassic rocks seem to be 0.1–0.3 Ga older than those of the southeastern ultrapotassic rocks. The southwestern Tibetan potassic rocks, in contrast to the uniform Nd isotopic composition for the southeastern and northern Tibetan potassic rocks, have highly variable εNd values of –9.5 to –16.6, and T_{DM} ages of 1.3 to 2.0 Ga (Miller et al., 1999). Nd modal ages may be interpreted as indicating the timing of the metasomatism event in the SCLM (Turner et al., 1996). However, they may more likely be ascribed to represent an average residence time for sediments that had been involved into the SCLM source by pre-existing subduction. Therefore, the difference in Nd isotopes observed in potassic and ultrapotassic magmas from northern (<15 Ma), southwestern (25–17 Ma), and southeastern (40–30 Ma) parts of the Tibetan Plateau suggest broadly contemporaneous mantle metasomatism by subducted sediments from different crustal environments.

Conclusions

The Late Paleogene lamprophyres from western Yunnan, disposed along the southeastern margin of the Tibetan Plateau, are mostly ultrapotassic in composition. They are characterized by enrichment in large-ion lithophile elements, light rare-earth elements, and Pb; depletion in high-field-strength elements; high initial $^{87}Sr/^{86}Sr$ ratios (0.70624–0.70924); and negative εNd(T) values (–1.7 to –4.6), resembling those of high-K/Ti, low-Ti potassic magmas formed in subduction-related settings. They were likely generated by partial melting of an evenly distributed metasomatized, phlogopite-bearing spinel harzburgite lithospheric mantle source, followed by crystal fractionation and varying degrees of crustal assimilation. The compositions of the SCLM beneath northern (<15 Ma), southwestern (25–17 Ma), and southeastern (40–30 Ma) parts of the Tibetan Plateau appear to be heterogeneous in geochemistry and Nd-Sr isotopes, as revealed by the potassic and ultrapotassic magmas. Such heterogeneity of the SCLM may be attributed to different timing of mantle metasomatism events and/or metasomatism by subducted sediments from distinct crustal provenances.

Acknowledgments

XHL thanks the Department of Geosciences, National Taiwan University for a six-month visiting

fellowship. This work was supported by the Chinese Academy of Sciences (grant KZCX2-102), Ministry of Science and Technology of China (grant 95-A-25), and the National Natural Science Foundation of China (grant 49725309).

REFERENCES

Arnaud, N., Vidal, Ph., Tapponnier, P., Matte, Ph., and Deng, W. M., 1992, The high K_2O volcanism of northwestern Tibet: geochemistry and tectonic implications: Earth and Planetetary Science Letters, v. 111, p. 355–367.

Bureau of Geology and Mineral Resources of Yunnan Province, 1990, Regional geology of Yunnan Province: Beijing, China, Geological Publishing House, 727 p.

Canning, J. C., Henney, P. J., Morrison, M. A., and Gaskarth, J. W., 1996, Geochemistry of late Caledonian minettes from Northern Britain: Implications for the Caledonian sub-continental lithospheric mantle: Mineralogical Magazine, v. 60, p. 221–236.

Chung, S. L., Lee, T. Y., Lo, C. H., Wang, P. L., Chen, C. Y., Yem, N. T., Huo, T., and Wu, G., 1997, Intraplate extension prior to continental extrusion along the Ailao Shan-Red River shear zone: Geology, v. 25, p. 311–314.

Chung, S. L., Lo, C. H., Lee, T. Y., Zhang, Y., Xie, Y. Li, X., Wang, K. L., and Wang, P. L., 1998, Diachronous uplift of the Tibetan plateau starting 40 Myr ago: Nature, v. 394, p. 769–773.

Foley, S. F., 1992, Petrological characterization of the source components of potassic magmas: Geochemical and experimental constraints: Lithos, v. 28, p. 187–204.

Gibson, S. A., Thompson, R. N., Leat, P. T., Morrison, M. A., Hendry, G. L., Dickin, A. P., and Mitchell, L. G., 1993, Ultrapotassic magmas along the flanks of the Oligo-Miocene Rio Grande Rift, U.S.A: Monitors of the zone of lithospheric mantle extension and thinning beneath a continental rift: Journal of Petrology, v. 34, p. 187–228.

Jahn, B. M., and Condie, K. C., 1995, Evolution of the Kaapvaal craton as viewed from geochemical and Sm-Nd isotopic analyses of intracratonic pelites: Geochimica et Cosmochimica Acta, v. 59, p. 2239–2258.

Lee, C. Y., Tsai, J. H., Ho, H. H., Yang, T. F., Chung, S. L., and Chen, C. H., 1997, Quantitative analysis in rock samples by an X-ray fluorescence spectrometer, (I) major elements [ext. abs.], *in* Annual Meeting of Geological Society of China, abstract volume, p. 418–420 (in Chinese).

Leloup, P. H., Lacassin, R., Tapponnier, P., Schärer, U., Zhong, D., Liu, X., Zhang, L., Ji, S., and Phan, T. T., 1995, The Ailao Shan–Red River shear zone (Yunnan, China), Tertiary transform boundary of Indochina: Tectonophysics, v. 251, p. 3–84.

Li, X. H., 1997, Geochemistry of the Longsheng Ophiolite from the southern margin of Yangtze Craton, SE China: Geochemical Journal, v. 31, p. 323–337.

McKenzie, D. P., 1989, Some remarks on the movement of small melt fractions in the mantle: Earth and Planetetary Science Letters, v. 95, p. 53–72.

Miller, C., Schuster, R., Klotzli, U., Frank, W., and Purtscheller, F., 1999, Post-collisional potassic and ultrapotassic magmatism in SW Tibet: Geochemical and Sr-Nd-Pb-O isotopic constraints for mantle source characteristics and petrogenesis: Journal of Petrology, v. 40, p. 1399–1424.

Müller, D., and Groves, D., 1993, Direct and indirect associations between potassic igneous rocks, shoshonites, and gold-copper deposits: Ore Geology Review, v. 8, p. 383–406.

Rogers, N. W., 1992, Potassic magmatism as a key to trace-element enrichment processes in the upper mantle: Journal of Volcanology and Geothermal Research, v. 50, p. 85–99.

Rogers, N. W., James, D., Kelley, S. P., and De Mulder, M., 1998, The generation of potassic lavas from the eastern Virunga province, Rwanda: Journal of Petrology, v. 39, p. 1223–1247.

Sheppard, S., and Taylor, W. R., 1992, Barium- and LREE-rich, olivine-mica-lamprophyres with affinities to lamproites, Mt. Bundey, Northern Territory, Australia: Lithos, v. 28, p. 303–325.

Sun, S.-S., and McDonough, W. F., 1989, Chemical and isotopic systematics of oceanic basalt: Implications for mantle composition and processes, *in* Saunders, A. D. and Norry, M. J., eds., Magmatism in the ocean basins: Geological Society of London Special Publication 42, p. 528–548.

Tapponnier, P., Peltzer, G., Armijo, R., Le Dain, A.-Y., and Cobbold, P., 1982, Propagating extrusion tectonics in Asia: New insights from simple experiments with plasticine: Geology, v. 10, p. 611–616.

Taylor, S. R., and McLennan S. M., 1985, The continental crust: Its composition and evolution: Oxford, UK, Blackwell Science Publications, 312 p.

Turner, S., Arnaud, N., Liu, J., Rogers, N., Hawkesworth, C., Harris, N., Kelley, S., Van Calsteren, P., and Deng, W., 1996, Post-collision, shoshonitic volcanism on the Tibetan plateau: Implications for convective thinning of the lithosphere and the source of ocean island basalts: Journal of Petrology, v. 37, p. 45–71.

Turner, S., Hawkesworth, C., Liu, J., Rogers, N., Kelley, S., and Van Calsteren, P., 1993, Timing of Tibetan uplift constrained by analysis of volcanic rocks: Nature, v. 364, p. 50–53.

Wang, P.-L., Lo, C.-H., Lee, T.-Y., Chung, S.-L., Lan, C.-Y., and Yem, N.T., 1998, Thermochronological evidence for the movement of the Ailao Shan–Red River Shear Zone: A perspective from Vietnam: Geology, v. 26, p. 887–890.

Williams, R., and Gill, J. B., 1989, Effects of partial melting on the uranium decay series: Geochimica et Cosmochimica Acta, v. 53, p. 1607–1619.

Wyllie, P. J., and Sekine, T., 1982, The formation of mantle phlogopite in subduction zone hybridization: Contributions to Mineralogy and Petrology, v. 79, p. 375–380.

Zhang, Y. Q., Xie, Y. W., and Tu, G. Z., 1987, Preliminary studies of the alkali-rich intrusive rocks in the Ailaoshan-Jinshajiang belt and their bearing on rift tectonics: Acta Petrologica Sinica, v. 3, p. 17–26 (in Chinese with English abstract).

Zhao, J.-X., Shiraishi, K., Ellis, D. J., and Sheraton, J. W., 1995, Geochemical and isotopic studies from the Yamato Mountains, East Antarctica: Implications for the origin of syenitic magmas: Geochimica et Cosmochimica Acta, v. 59, p. 1363–1382.

Zhu, B. Q., Zhang, Y. Q., and Xie, Y. W., 1992, Isotope characteristics of Cenozoic potassic volcanic rocks from Haidong,Yunnan, and their implications for subcontinental mantle evolution in southwestern China: Geochimica, v. 21, p. 201–212 (in Chinese with English abstract).